Article

Discovery Medicine 2026; 38(205): 468–481
https://doi.org/10.24976/Discov.Med.202638205.39

CaMKIα-Driven Regulation of the AMPK/SIRT3 Pathway in Controlling Inflammatory Responses During Acute Lung Injury

Lina Zheng[1], Bin Zhang[1], Lingzhi Zhao[1], Pengfei Zhang[2,*]

[1]Department of Pediatrics, The Affiliated Yueqing Hospital of Wenzhou Medical University, 325600 Wenzhou, Zhejiang, China
[2]Department of Respiratory and Critical Care Medicine, The Third Affiliated Hospital of Wenzhou Medical University, 325200 Wenzhou, Zhejiang, China
*Correspondence: 251689188@qq.com (Pengfei Zhang)
Submitted: 24 November 2025 Revised: 25 December 2025 Accepted: 5 January 2026 Published: 20 February 2026

Background: To investigate the role and the underlying mechanisms of Calcium/calmodulin-dependent protein kinase Iα (CaMKIα) in modulating inflammatory responses during acute lung injury (ALI) via the AMPK/Sirtuin 3 (SIRT3) signaling pathway.

Methods: Neonatal rats were intratracheally administered Lipopolysaccharide (LPS) to induce ALI, while L2 alveolar epithelial cells were treated with LPS (100 ng/mL) *in vitro*. CaMKIα expression was silenced using siRNA in L2 cells and via AAV2/9-shRNA in rats. AMP-activated protein kinase (AMPK) activity was inhibited with Compound C (5 μM) *in vitro*. Pulmonary histopathology, bronchoalveolar lavage fluid cytokine levels, and key AMPK/SIRT3 pathway protein expressions were assessed.

Results: CaMKIα knockdown significantly alleviated lung injury in ALI rats, and significantly reduced lung edema, inflammatory cytokine levels, and histological injury (all $p < 0.05$). *In vitro*, CaMKIα knockdown enhanced L2 cell viability, suppressed apoptosis, and reduced pro-inflammatory cytokine production (all $p < 0.05$) via AMPK/SIRT3 activation. Inhibition of AMPK with Compound C abolished these protective effects ($p < 0.05$), confirming the involvement of this pathway.

Conclusion: CaMKIα attenuates inflammatory responses in ALI through activation of the AMPK/SIRT3 axis, indicating it may serve as a promising target for ALI therapy.

Keywords: CaMKIα; AMPK/SIRT3; acute lung injury; inflammatory response

Introduction

Acute lung injury (ALI) represents a rapid inflammatory reaction in the lungs caused by diverse pathological stimuli and is often considered an early or mild form of acute respiratory distress syndrome (ARDS). It mainly affects alveolar epithelial cells and pulmonary capillary endothelial cells, resulting in widespread structural changes in lung tissue, progressive respiratory compromise, and persistent hypoxemia. ALI is a severe condition that can affect individuals of all ages, with neonates—especially preterm infants—being particularly vulnerable and exhibiting relatively high mortality [1–3]. The development of neonatal ALI is multifactorial, with dysregulated inflammatory responses serving as a key contributor. Excessive inflammatory responses damage alveolar epithelial and capillary endothelial cells, resulting in increased permeability of the alveolar-capillary barrier. This process impairs gas exchange, while inflammatory exudates within the alveoli reduce the activity of pulmonary surfactant, increase alveolar surface tension, exacerbate pulmonary edema, reduce lung compliance, and further deteriorate pulmonary function [4]. To date, the underlying mechanisms of neonatal ALI remain incompletely elucidated. Conventional therapeutic strategies mainly focus on addressing the underlying cause, correcting hypoxemia, and supporting organ function [5,6]. However, these approaches are insufficient to halt the pathological progression of ALI or promote repair of injured lung cells. Thus, the development of novel and effective therapeutic strategies is urgently needed.

AMP-activated protein kinase (AMPK) functions as a key regulator of cellular energy balance and stress responses. Its activation promotes autophagy and suppresses inflammation [7]. In animal models of ALI, AMPK activation has been shown to significantly alleviate inflammatory cell infiltration and lung tissue injury [8]. Likewise, sirtuin 3 (SIRT3) is crucial for controlling inflammation. Upregulation of SIRT3 promotes autophagy through the AMPK/mTOR pathway, consequently suppressing inflammatory responses [9]. Accumulating evidence suggests that activation of AMPK/SIRT3 pathway alleviates multiple inflammation-related pathologies, including ALI, highlighting its potential as a therapeutic target for inflammatory disorders [10].

Calcium/calmodulin-dependent protein kinase Iα (CaMKIα) is a downstream effector of calcium signaling that can phosphorylate AMPK and promote autophagy, thereby playing an important role in inflammation regulation [11]. Previous studies have demonstrated that CaMKIα activation induces ATG7-dependent autophagy, suppresses excessive inflammation, and alleviates LPS-induced acute pulmonary inflammation [12]. However, these studies primarily focused on general AMPK-related pathways in inflammatory contexts and did not directly examine the AMPK/SIRT3 axis in acute lung injury [13,14]. Thus, our study extends previous findings by directly linking CaMKIα activity to AMPK/SIRT3-mediated modulation of inflammatory responses in ALI.

The present study aims to systematically investigate the role and underlying mechanisms of CaMKIα in regulating the AMPK/SIRT3 signaling pathway during ALI. Specifically, we sought to verify the regulatory effect of CaMKIα on the AMPK/SIRT3 axis in ALI models and to elucidate the critical mechanisms by which CaMKIα modulates inflammatory responses via this pathway. These findings are expected to provide a theoretical basis and potential molecular targets for novel therapeutic strategies against ALI.

Materials and Methods

Animals

Adult Sprague-Dawley (SD) rats were obtained from Speifu Biotechnology Co., Ltd. (Beijing, China). A total of 30 adult rats (male: 20; female: 10; age: 8–10 weeks; body weight: 250–300 g) were housed at a male-to-female ratio of 1:2 for breeding under specific pathogen-free (SPF) conditions. Pregnant females were transferred to individual cages until natural delivery. After birth, 70 neonatal rats were randomly selected for subsequent experiments. Animals were maintained at 22–26 °C with 40–70% relative humidity and a 12-h light/dark cycle, with sterilized cages, bedding, and feed.

All neonatal rats were euthanized at the end of the experiment via intraperitoneal injection of pentobarbital sodium (150 mg/kg), and death was confirmed by cessation of heartbeat.

Grouping and Model Establishment

An adeno-associated virus (AAV) vector carrying shRNA targeting CaMKIα (AAV-shCaMKIα) and a negative control vector (AAV-NC) were purchased from PackGene (Guangzhou, China). The validated shRNA sequence targeting Camk1 was 5′-GGTGTCTGATATCAAGTTA-3′. A scrambled shRNA sequence with no homology to the rat genome was used as the negative control (AAV-NC). The viral titer was 1×10^{11} vg/mL. Neonatal rats received intratracheal administration of 20 µL virus suspension under light anesthesia. The AAV serotype used was AAV2/9, which exhibits preferential tropism for lung epithelial cells, resulting in predominant gene modulation in alveolar epithelial cells.

To validate successful establishment of the LPS-induced ALI model and to determine whether CaMKIα expression is altered during ALI, a preliminary model-validation experiment was performed. Neonatal rats were assigned to a Control group (saline without LPS), a Model group (saline + LPS), and a Model + KO-NC group (AAV-NC + LPS). CaMKIα expression in lung tissues and Bronchoalveolar Lavage Fluid (BALF) inflammatory indicators were assessed, confirming successful ALI induction and demonstrating comparable pathological changes between the Model and Model + KO-NC groups.

For mechanistic studies, neonatal rats were intratracheally injected with AAV-NC or AAV-shCaMKIα at one week of age. One week after viral transduction, ALI was induced by intranasal instillation of LPS (5 mg/kg, HY-D1056, MCE, NJ, USA). Based on this design, animals were divided into four groups: Ctrl group (AAV-NC without LPS), KO-CaMKIα group (AAV-shCaMKIα without LPS), ALI group (AAV-NC + LPS), and ALI + KO group (AAV-shCaMKIα + LPS). Body weight was recorded daily starting from the day of LPS administration. Bronchoalveolar lavage fluid (BALF) and lung tissues were collected seven days after LPS challenge for subsequent analyses.

Lung Wet-to-Dry Weight Ratio

After collecting BALF, the left (unlavaged) lung was removed and weighed to determine its wet weight. The lung tissue was subsequently dried in an oven at 80 °C for 48 hours until a stable weight was achieved. The dry weight was then measured, and the wet-to-dry (W/D) ratio of the lung was calculated to evaluate pulmonary edema.

BALF Total Cell Count and Total Protein Concentration

The total cell count in BALF was measured with a hemocytometer (Z359629, Merck, Darmstadt, DE). BALF samples were centrifuged at 3000 rpm for 10 minutes at 4 °C, and the resulting supernatant was collected to determine total protein content using a commercial assay kit (BCA Protein Assay Kit, Cat. No. BCA1, Merck, Darmstadt, DE) following the manufacturer's instructions.

Histological Analysis

Lung tissues were fixed in 4% paraformaldehyde (158127, Sigma-Aldrich, MI, USA), embedded in paraffin, and sectioned at a thickness of 4 µm. Sections were deparaffinized in xylene and rehydrated through a graded ethanol series (100%, 95%, 80%, and 70%). Histopathological changes, including inflammation and fibrosis, were assessed using hematoxylin and eosin (HE) staining (C0105S, Beyotime, Shanghai, China) and Masson's trichrome staining (HT15, Sigma-Aldrich, MI, USA).

Table 1. Primer sequences used for qRT-PCR.

Gene	Forward sequence (5′-3′)	Reverse sequence (5′-3′)
CaMKIα	TGTGGCGTCATCCTGTATATCTTG	CCTTCACGCCATCATTCTTCTTG
TNF-α	GCCCACGTCGTAGCAA	GTCTTTGAGATCCATG
IL-6	TCCTACCCCAACTTCCAATGCTC	TTGGATGGTCTTGGTCCTTAGCC
IL-10	CAGAAATCAAGGAGCATTTG	CTGCTCCACTGCCTTGCTTT
IL-1β	CACCTCTCAAGCAGAGCACAG	GGGTTCCATGGTGAAGTCAAC
β-actin	GAAGATCAAGATCATTGCTCCT	TACTCCTGCTTGCTGATCCA

qRT-PCR, Quantitative Real-Time Polymerase Chain Reaction.

Table 2. Primary antibodies used in this study.

Antibody	Brand	Catalog number	Dilution ratio
CaMKIα	Abcam, Cambridge, UK	ab68234	1:5000
NF-κB	Proteintech, IL, USA	80979-1-RR	1:5000
NLRP3	Abcam	ab263899	1:1000
COX-2	Abcam	ab179800	1:1000
iNOS	Abcam	ab178945	1:1000
p-AMPK	Abcam	ab133448	1:1000
AMPK	Abcam	ab32047	1:1000
SIRT3	Abcam	ab246522	1:1000
β-actin	Abcam	ab8226	1:1000

Abbreviations: CaMKIα, Calcium/Calmodulin-Dependent Protein Kinase Iα; NF-κB, Nuclear Factor kappa-light-chain-enhancer of activated B cells; NLRP3, NOD-, LRR- and pyrin domain-containing protein 3; COX-2, Cyclooxygenase-2; iNOS, Inducible Nitric Oxide Synthase; p-AMPK, Phosphorylated AMP-Activated Protein Kinase; SIRT3, Sirtuin 3.

For HE staining, sections were stained with hematoxylin for 5–8 min, rinsed, differentiated in 1% acid alcohol, blued in tap water, and counterstained with eosin for 1–3 min. For Masson's trichrome staining, sections were sequentially stained with Weigert iron hematoxylin for 5–10 min, followed by Biebrich scarlet-acid fuchsin for 5–10 min. Sections were then differentiated in phosphomolybdic/phosphotungstic acid solution until collagen staining eliminated, and subsequently counterstained with aniline blue for 5–10 min. After staining, all sections were dehydrated, cleared, and mounted with neutral resin for imaging.

All staining procedures were performed according to the manufacturers' instructions and optimized based on kit protocols to ensure reproducibility.

Cell Culture and Stimulation

Rat alveolar type II epithelial cells (L2 cells, SNP-R122, SUNNCELL, Wuhan, China) were maintained in RPMI (R8758, Merck, Darmstadt, DE) medium containing 10% fetal bovine serum (FBS, 12103C, Merck, Darmstadt, DE) and 1% penicillin-streptomycin (P4333, Merck, Darmstadt, DE) under standard culture conditions (37 °C, 5% CO_2). L2 alveolar epithelial cells were routinely tested and confirmed to be mycoplasma-free before use. Cell identity was confirmed by morphological observation and SP-C immunofluorescence staining. To establish an *in vitro* ALI model, cells were exposed to LPS (100 ng/mL) [15]. CaMKIα expression was silenced using siRNA transfection, with a negative control (NC) group included to eliminate nonspecific effects. Knockdown efficiency was confirmed by Western blotting. In selected groups, cells were additionally treated with the AMPK-specific inhibitor Compound C (P5499, Merck, Darmstadt, DE, final concentration 5 μM) to block AMPK activation and detect its role in CaMKIα-mediated regulation of inflammation.

Cell Viability Assay

Cell viability was assessed using the Cell Counting Kit-8 (CCK-8, C0038, Beyotime, Shanghai, China). Cells were seeded in 96-well plates (CLS3600, Merck, Darmstadt, DE) at a density of approximately 5×10^3 cells per well (100 μL/well) in triplicate. After treatment, 10 μL of CCK-8 solution was added to each well, followed by incubation for 2 h at 37 °C in 5% CO_2. Absorbance at 450 nm was measured with a microplate reader, and optical density (OD) values were used to quantify cell viability. The mean values were calculated for subsequent statistical analysis.

Cell Apoptosis Assay

Apoptotic cells were detected using a Terminal deoxynucleotidyl transferase dUTP nick end labeling (TUNEL) staining kit (11684795910, Roche Diagnostics, IN, USA) and observed under a fluorescence microscope.

Measurement of Inflammatory Cytokines by Enzyme-Linked Immunosorbent Assay (ELISA)

BALF and cell culture supernatants were centrifuged at 3000 rpm for 10 minutes at 4 °C. Concentrations of Tumor Necrosis Factor-alpha (TNF-α), Interleukin-6 (IL-6), Interleukin-10 (IL-10), and Interleukin-1 beta (IL-1β) were quantified using ELISA kits (EK0527, EK0411, EK0418, EK0394; Wuhan Boster Biological Technology Co., Wuhan, China) following the manufacturer's instructions.

RNA Extraction and Quantitative Real-Time Polymerase Chain Reaction (qRT-PCR)

Total RNA was isolated from lung tissues and L2 cells using TRIzol reagent (15596018, Thermo Fisher Sci-

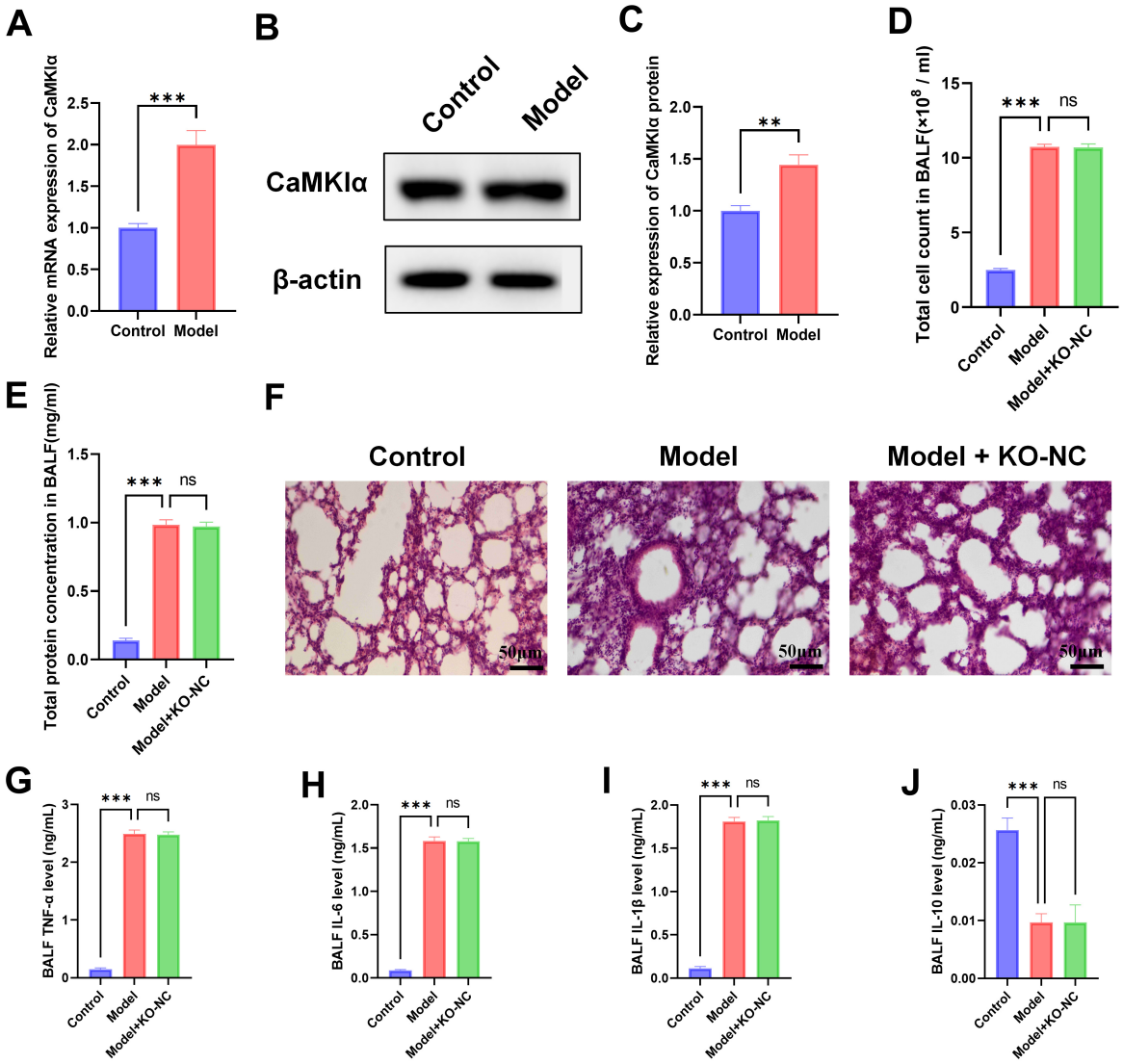

Fig. 1. Validation of ALI model establishment and CaMKIα expression in neonatal rats. (A) qRT-PCR analysis of CaMKIα mRNA expression in lung tissues. (B,C) Western blot analysis of CaMKIα protein expression and corresponding densitometric quantification. (D) Total cell count in BALF. (E) Total protein concentration in BALF. (F) Representative lung histological staining. (G–J) BALF levels of inflammatory cytokines TNF-α, IL-6, IL-1β, and IL-10 measured by ELISA. n = 5. ***$p < 0.001$, **$p < 0.01$, $^{ns}p > 0.05$. ALI, acute lung injury; BALF, Bronchoalveolar Lavage Fluid; TNF-α, Tumor Necrosis Factor-alpha; IL-6, Interleukin-6; IL-10, Interleukin-10; IL-1β, Interleukin-1 beta; ELISA, Enzyme-Linked Immunosorbent Assay.

entific, MA, USA) and subsequently treated with DNase I (11284932001, Sigma-Aldrich, MI, USA). cDNA was synthesized from 1 µg of RNA using the High-Capacity cDNA Reverse Transcription Kit (4368814, Thermo Fisher Scientific, Waltham, MA, USA). Quantitative PCR was performed with a qRT-PCR kit (11732088, Thermo Fisher Scientific, Waltham, MA, USA), and relative mRNA levels were normalized to β-actin using the $2^{-\Delta\Delta Ct}$ method. Primer sequences are provided in Table 1.

Western Blotting

Total protein was isolated from rat lung tissues and L2 cells using RIPA (R0278, Merck, Darmstadt, DE) lysis buffer, and concentrations were measured with a BCA Protein Assay Kit (P0012, Beyotime, Shanghai, China). Equal amounts of protein (20 µg per lane) were resolved by polyacrylamide gel electrophoresis (PAGE) and transferred onto PVDF (IESN07852, Merck, Darmstadt, DE) membranes. Membranes were blocked with 5% non-fat milk for 1 h at room temperature and then incubated overnight at 4 °C with the designated primary antibodies (Table 2). After washing with TBST, membranes were incubated with Horseradish Peroxidase (HRP)-conjugated secondary antibodies (goat anti-rabbit IgG-HRP, ab6721, Abcam, 1:2000; goat anti-mouse IgG-HRP, ab205719, Abcam, 1:2000) at room temperature for 1 hour. Protein bands were detected using a

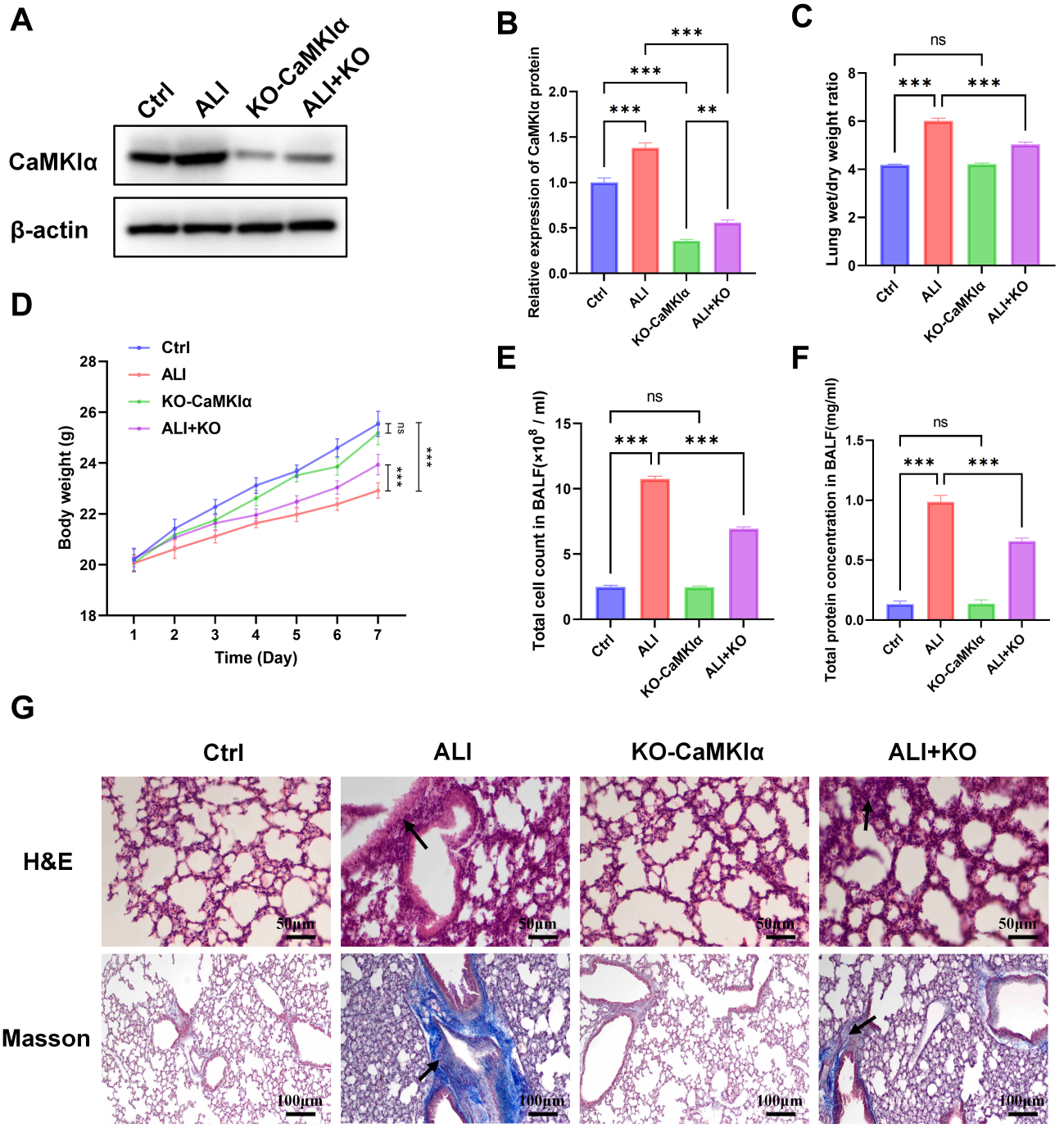

Fig. 2. Effect of CaMKIα knockdown on pulmonary function in ALI rats. (A,B) Validation of CaMKIα knockdown by Western blotting. (C) Lung wet/dry weight ratio. (D) Body weight changes. (E) Total BALF cell counts. (F) BALF total protein concentration. (G) Histological changes in lung tissue; arrows indicate inflammatory infiltration. Hematoxylin and Eosin (H&E) staining: magnification, 200×; Masson staining: magnification, 100×. n = 5. ***$p < 0.001$, **$p < 0.01$, $^{ns}p > 0.05$.

ChemiDoc XRS+ imaging system (Bio-Rad, Hercules, CA, USA), and relative protein levels were quantified with ImageJ Pro-Plus 6.0 software (Tanon, Shanghai, China).

Statistical Analysis

Data are presented as the mean ± SEM. Statistical analyses were conducted using GraphPad Prism version 7.0 (GraphPad Software, San Diego, CA, USA). Comparisons between control and treatment groups were performed using two-way analysis of variance (ANOVA) followed by Tukey's post hoc test. Statistical significance was defined solely as a $p < 0.05$.

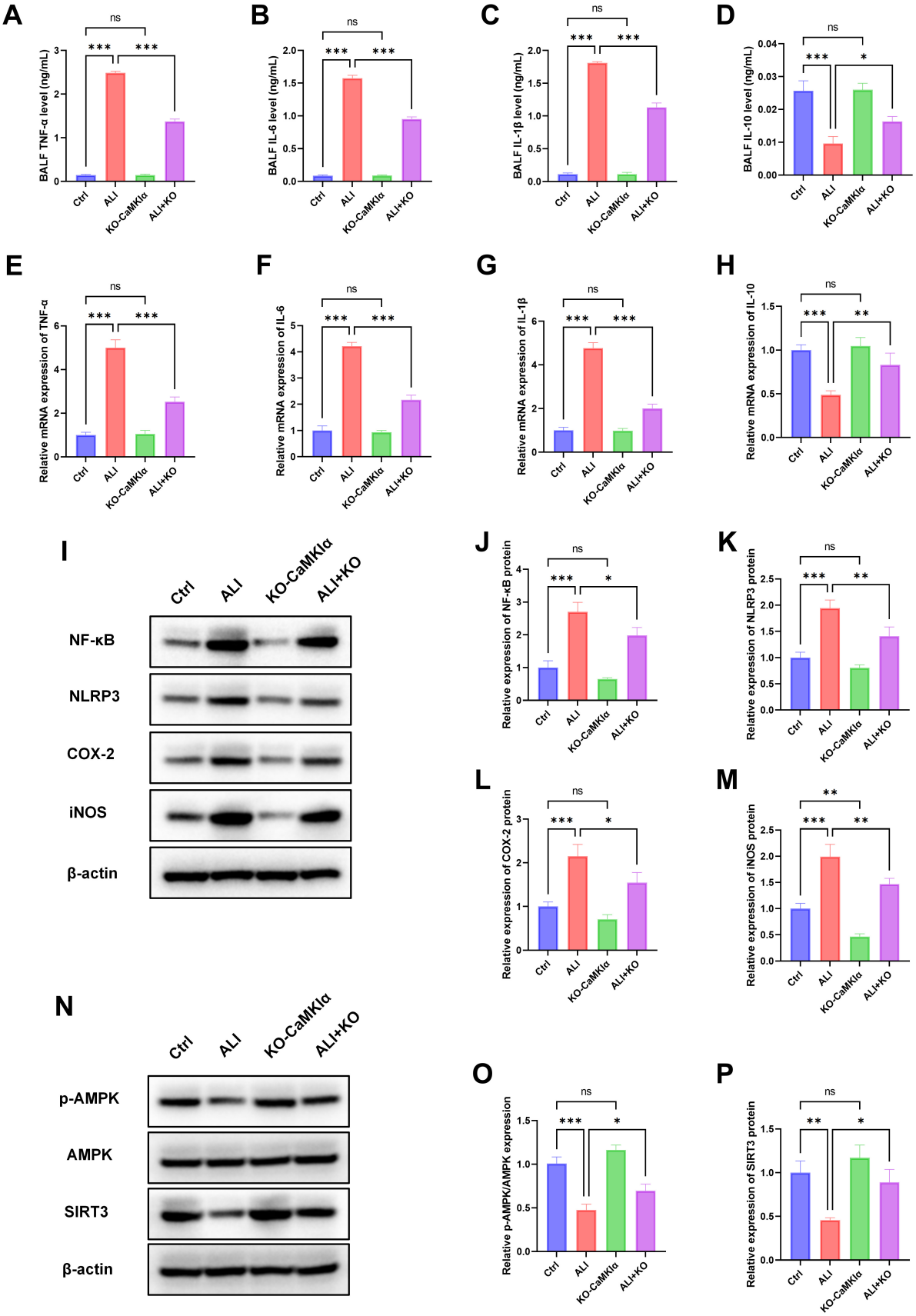

Fig. 3. Mechanisms underlying the effects of CaMKIα knockdown on pulmonary inflammation. (A–D) BALF cytokine levels (TNF-α, IL-6, IL-1β, IL-10). (E–H) mRNA levels of cytokines in lung tissue. (I–M) Protein expression of NF-κB, NLRP3, COX-2, and iNOS. (N–P) Protein levels of p-AMPK, AMPK, and SIRT3. n = 5. ***$p < 0.001$, **$p < 0.01$, *$p < 0.05$, $^{ns}p > 0.05$.

Results

CaMKIα Is Upregulated in LPS-Induced ALI and Validation of ALI Model Establishment

qRT-PCR analysis revealed that CaMKIα mRNA expression was significantly increased in lung tissues of the Model group compared with the Control group ($p < 0.01$, Fig. 1A). Consistently, Western blot analysis demonstrated a marked upregulation of CaMKIα protein levels in ALI rats, as evidenced by quantitative densitometric analysis (Fig. 1B,C).

To further verify successful ALI model establishment, BALF was collected and analyzed. The total cell count and total protein concentration in BALF were significantly elevated in the Model group compared with the Control group ($p < 0.01$), indicating increased inflammatory cell infiltration and alveolar-capillary barrier disruption (Fig. 1D,E). No significant differences were detected between the Model and Model + KO-NC groups.

Histological examination revealed pronounced alveolar damage and inflammatory cell infiltration in the Model group compared with the Control group, which showed preserved lung architecture (Fig. 1F). Similar histopathological alterations were observed in the Model + KO-NC group, suggesting no obvious impact of the control vector on LPS-induced lung injury. In addition, ELISA results demonstrated that pro-inflammatory cytokines TNF-α, IL-6, and IL-1β were significantly increased, while the anti-inflammatory cytokine IL-10 was decreased in the BALF of Model rats compared with Controls ($p < 0.001$), while no significant differences were observed between the Model and Model + AAV-NC groups (Fig. 1G–J).

Knockdown of CaMKIα Improves Pulmonary Function in ALI Rats

Western blotting demonstrated a significant upregulation of CaMKIα in the ALI group ($p < 0.001$), whereas its expression was markedly decreased in both the KO-CaMKIα and ALI+KO groups, confirming effective gene silencing (Fig. 2A,B, $p < 0.001$). Functionally, ALI rats showed a higher lung wet/dry ratio ($p < 0.001$), reduced body weight gain ($p < 0.001$), and increased BALF cell counts and protein levels (Fig. 2C–F, $p < 0.001$). These pathological alterations were notably ameliorated after CaMKIα knockdown ($p < 0.05$, $p < 0.001$). Consistently, histological evaluation revealed extensive inflammatory infiltration and alveolar injury in ALI lungs, which were substantially alleviated by CaMKIα silencing (Fig. 2G).

Knockdown of CaMKIα Suppresses Pulmonary Inflammation and Activates the AMPK/SIRT3 Pathway in ALI Rats

In the ALI group, TNF-α, IL-6, and IL-1β levels in BALF were significantly elevated, while IL-10 was reduced ($p < 0.001$). These alterations were reversed by CaMKIα knockdown (Fig. 3A–D, $p < 0.05$, $p < 0.001$). qRT-PCR results confirmed consistent trends in lung tissue mRNA expression (Fig. 3E–H). Protein analysis further demonstrated that nuclear Factor kappa-light-chain-enhancer of activated B cells (NF-κB), NOD-, LRR- and pyrin domain-containing protein 3 (NLRP3), cyclooxygenase-2 (COX-2), and inducible nitric oxide synthase (iNOS) were markedly upregulated in ALI rats ($p < 0.001$), but downregulated upon CaMKIα knockdown (Fig. 3I–M, $p < 0.05$, $p < 0.01$). Importantly, CaMKIα knockdown promoted the expression of p-AMPK and SIRT3 ($p < 0.05$, $p < 0.01$), suggesting that its anti-inflammatory effects may be mediated through the AMPK/SIRT3 signaling pathway (Fig. 3N–P).

CaMKIα Knockdown Enhances Cell Viability and Reduces Apoptosis in L2 Cells

In vitro, LPS stimulation significantly increased CaMKIα expression in L2 cells ($p < 0.05$), while siRNA-mediated knockdown effectively reduced its expression (Fig. 4A,B, $p < 0.001$). CCK-8 assays showed that LPS markedly decreased cell viability ($p < 0.01$), which was restored upon CaMKIα knockdown (Fig. 4C, $p < 0.05$). TUNEL staining revealed increased apoptosis after LPS treatment ($p < 0.001$), whereas CaMKIα knockdown substantially reduced apoptosis (Fig. 4D,E, $p < 0.001$).

CaMKIα Knockdown Attenuates L2 Cell Inflammation and Activates the AMPK/SIRT3 Pathway

LPS exposure markedly increased TNF-α, IL-6, and IL-1β secretion while reducing IL-10 in L2 cell supernatants (all $p < 0.001$). These cytokine changes were effectively reversed by CaMKIα knockdown (Fig. 5A–D, $p < 0.05$-0.001). Consistent results were obtained at the transcriptional level by qRT-PCR (Fig. 5E–H). Western blotting further showed that LPS robustly upregulated expression levels of NF-κB, NLRP3, COX-2, and iNOS ($p < 0.001$), whereas CaMKIα silencing significantly suppressed these protein levels (Fig. 5I–M, $p < 0.05$-0.001). In parallel, knockdown of CaMKIα promoted phosphorylation of AMPK and enhanced SIRT3 expression (Fig. 5N–P, $p < 0.05$–0.01).

Inhibition of the AMPK/SIRT3 Pathway Abolishes the Protective Effects of CaMKIα Knockdown on L2 Cells

To validate pathway involvement, L2 cells were treated with the AMPK inhibitor Compound C, which significantly suppressed p-AMPK and SIRT3 expression (Fig. 6A–C, $p < 0.001$). Functionally, inhibition of AMPK diminished the restoration of cell viability induced by CaMKIα knockdown and markedly increased apoptosis (Fig. 6D–F, $p < 0.05$, $p < 0.001$), indicating that the protective effects of CaMKIα knockdown are mediated through the AMPK/SIRT3 signaling pathway.

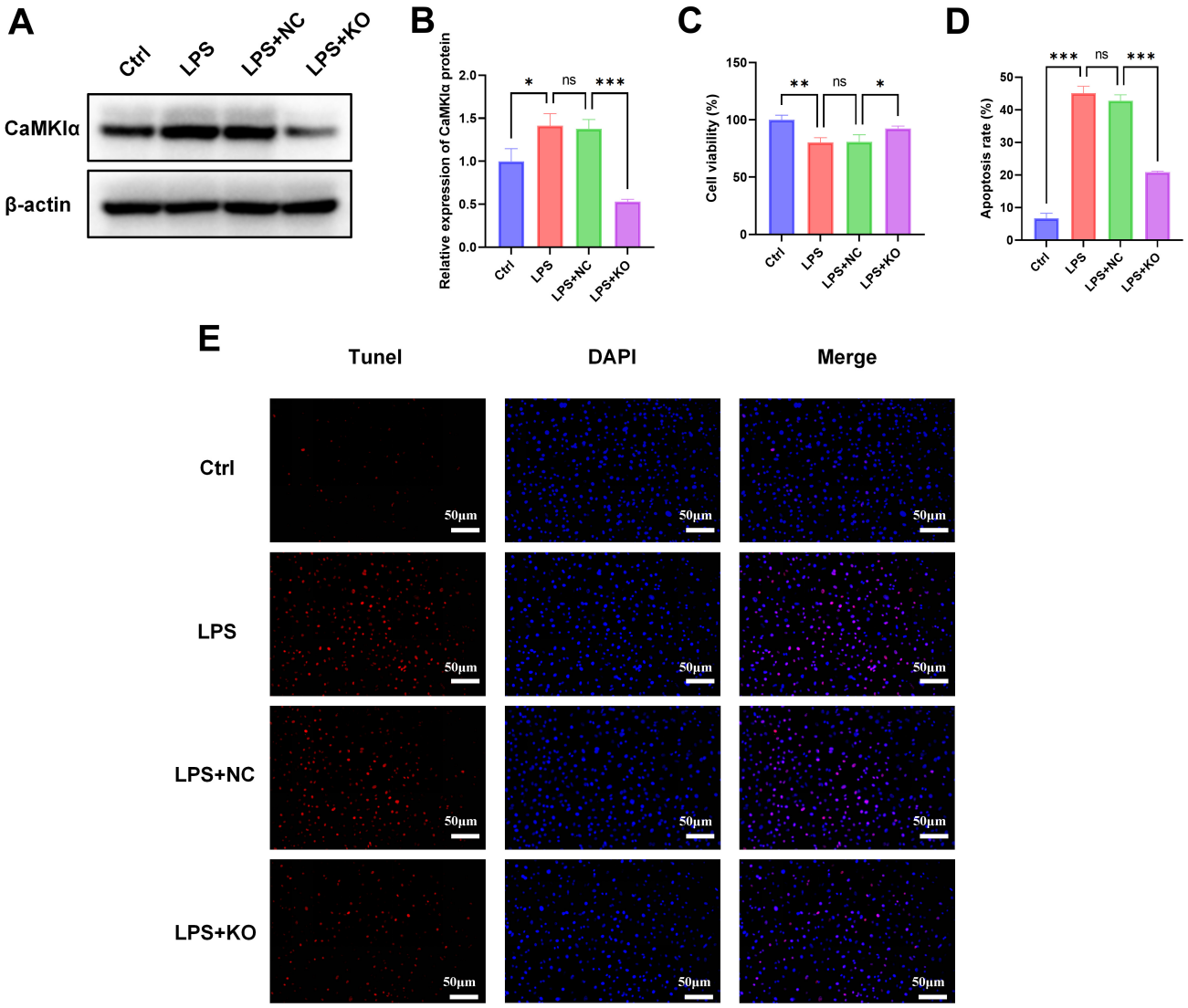

Fig. 4. Validation of CaMKIα knockdown efficiency and its effects on viability and apoptosis in L2 cells. (A,B) Western blot validation of CaMKIα knockdown. (C) Cell viability assessed by Cell Counting Kit-8 (CCK-8). (D,E) Apoptosis analysis by TUNEL staining and fluorescence quantification (magnification, 200×). n = 3. ***$p < 0.001$, **$p < 0.01$, *$p < 0.05$, $^{ns}p > 0.05$. TUNEL, Terminal deoxynucleotidyl transferase dUTP nick end labeling.

Inhibition of the AMPK/SIRT3 Pathway Attenuates the Anti-Inflammatory Effects of CaMKIα Knockdown

Cytokine profiling showed that LPS stimulation markedly elevated TNF-α, IL-6, and IL-1β levels while suppressing IL-10 (all $p < 0.001$). These changes were significantly ameliorated by CaMKIα knockdown ($p < 0.001$). In contrast, co-treatment with the AMPK inhibitor Compound C abrogated this protection, resulting in higher pro-inflammatory cytokines and further reduction of IL-10 (Fig. 7A–D, $p < 0.05$-0.001). Similar trends were confirmed at the mRNA level (Fig. 7E–H). Western blotting further demonstrated that CaMKIα silencing downregulated NF-κB, NLRP3, COX-2, and iNOS expression levels ($p < 0.001$), whereas these inhibitory effects were significantly attenuated by AMPK blockade (Fig. 7I–M, $p < 0.05$-0.01). Taken together, these results indicate that CaMKIα exerts anti-inflammatory protection through the AMPK/SIRT3 pathway, and this effect is largely abolished when AMPK activity is inhibited.

Discussion

ALI and its severe form, ARDS, are serious critical conditions marked by widespread damage to alveolar epithelial and endothelial cells, extensive infiltration of inflammatory cells, and overproduction of pro-inflammatory cytokines [16,17]. These pathological alterations ultimately compromise the alveolar-capillary barrier and impair oxygenation [18]. Although the underlying mechanisms have been partially elucidated, effective targeted

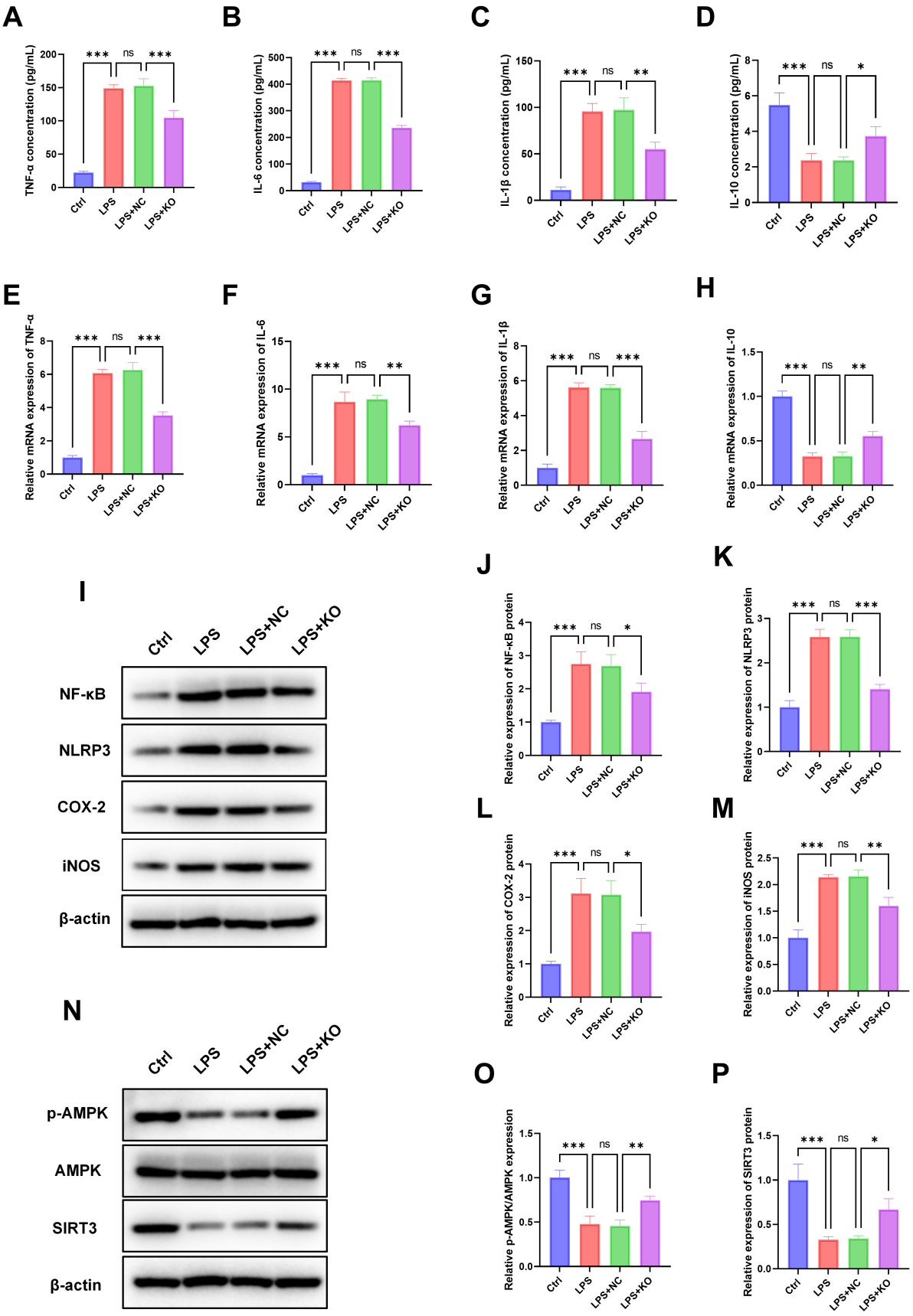

Fig. 5. Effects of CaMKIα knockdown on L2 cell inflammation. (A–D) Cytokine levels in cell supernatants. (E–H) Cytokine mRNA expression in L2 cells. (I–M) Protein expression of NF-κB, NLRP3, COX-2, and iNOS. (N–P) Protein levels of p-AMPK, AMPK, and SIRT3. n = 3. ***$p < 0.001$, **$p < 0.01$, *$p < 0.05$, $^{ns}p > 0.05$.

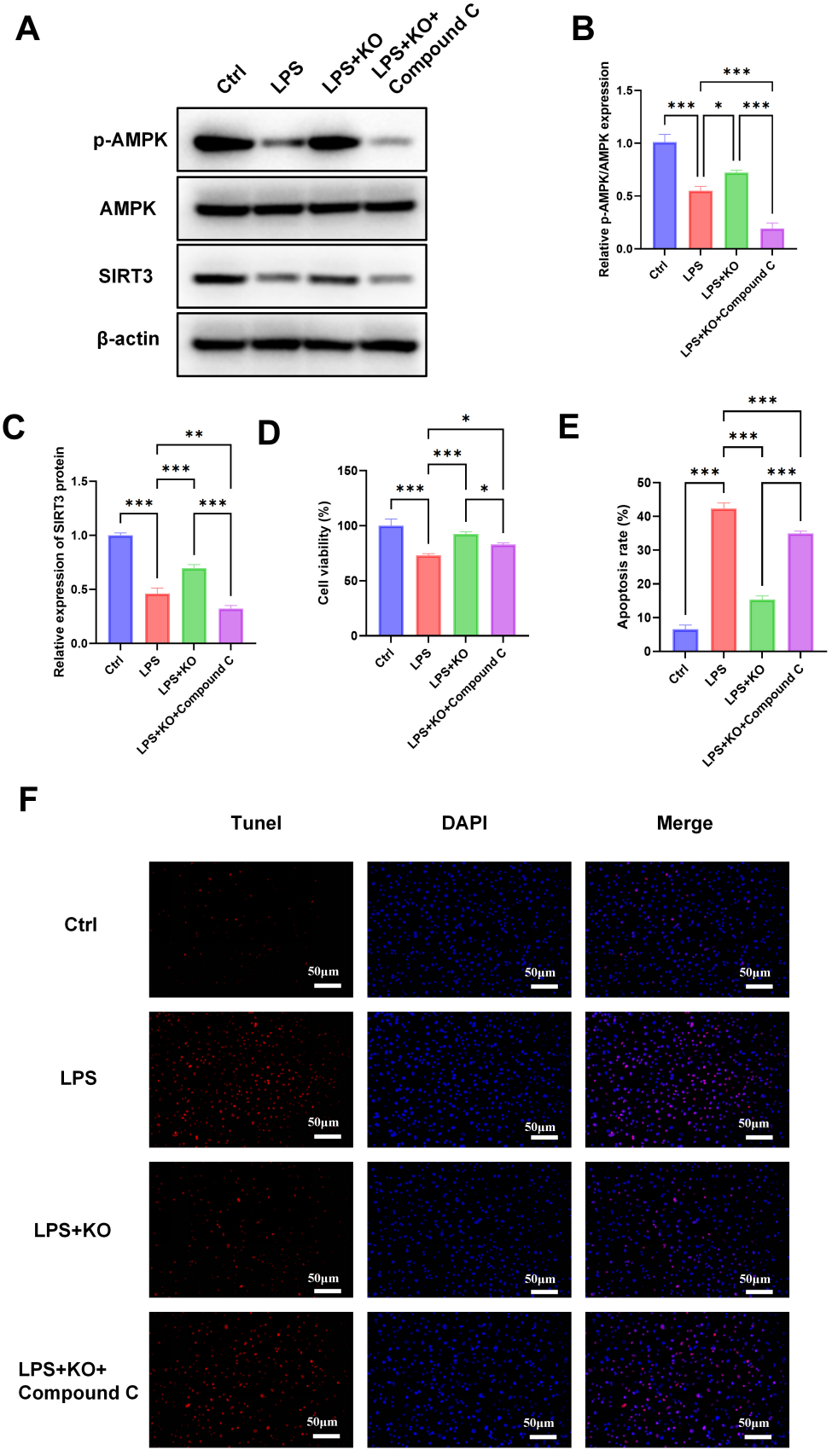

Fig. 6. Validation of AMPK/SIRT3 inhibition and its effects on viability and apoptosis in L2 cells. (A–C) Western blot validation of AMPK/SIRT3 inhibition. (D) Cell viability assessed by CCK-8. (E,F) Apoptosis analysis by TUNEL staining and fluorescence quantification (magnification, 200×). n = 3. ***$p < 0.001$, **$p < 0.01$, *$p < 0.05$.

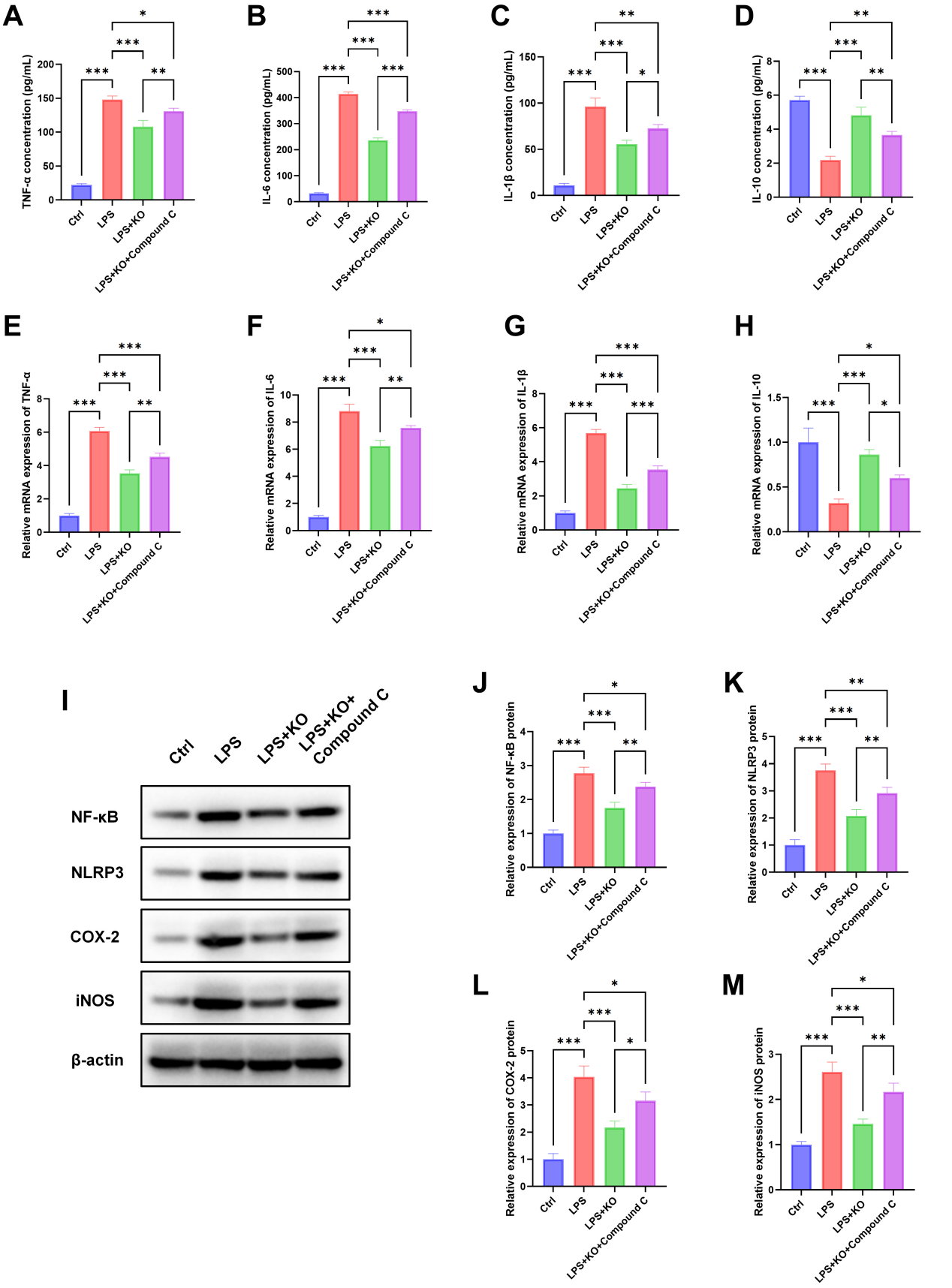

Fig. 7. Effects of AMPK/SIRT3 pathway inhibition on inflammatory responses in L2 cells. (A–D) Cytokine levels (TNF-α, IL-6, IL-1β, IL-10) in cell supernatants. (E–H) mRNA expression of cytokines in L2 cells. (I–M) Protein expression of NF-κB, NLRP3, COX-2, and iNOS assessed by Western blotting. n = 3. ***$p < 0.001$, **$p < 0.01$, *$p < 0.05$.

therapies remain limited [19]. Therefore, identifying novel molecular regulatory nodes is crucial for understanding the inflammatory mechanisms of ALI and exploring potential therapeutic targets. In this study, we employed a neonatal rat LPS-induced ALI model and L2 cells to systematically investigate the role of CaMKIα in inflammatory responses and its relationship with the AMPK/SIRT3 signaling pathway. Our results demonstrated that LPS stimulation induced upregulation of CaMKIα, whereas AAV-shRNA- or siRNA-mediated knockdown of CaMKIα markedly alleviated lung injury, reduced inflammation and apoptosis, and restored AMPK phosphorylation and SIRT3 expression. Further experiments using AMPK inhibition indicated that AMPK activation is essential for the protective effects of CaMKIα knockdown. Collectively, these findings suggest that CaMKIα may promote inflammation by negatively regulating the AMPK/SIRT3 pathway, and its knockdown relieves this inhibition to exert anti-inflammatory protection.

Upregulation and Biological Significance of CaMKIα in ALI

We found that CaMKIα was significantly upregulated in both the LPS-induced neonatal rat ALI model and L2 cells, and that knockdown of CaMKIα improved pulmonary function, mitigated inflammation and apoptosis. As a downstream effector of calcium signaling, CaMKIα has been implicated in the regulation of inflammation, cell death, and metabolic reprogramming, particularly in connection with the canonical AMPK pathway [11,20]. Our findings indicate that CaMKIα contributes to inflammatory responses in ALI by regulating the AMPK/SIRT3 axis, revealing a previously unrecognized link between calcium signaling and energy-sensing pathways in inflammation. Notably, while the CaMKIα-AMPK pathway has been implicated in inflammation, this study is the first to show that CaMKIα knockdown alleviates LPS-induced acute lung injury through the AMPK/SIRT3 axis in neonatal rats and alveolar epithelial cells, highlighting a novel upstream regulatory mechanism and potential therapeutic target. However, our conclusions are based on functional evidence, as direct molecular interactions between CaMKIα and AMPK/SIRT3 components have not been demonstrated. Future studies using co-immunoprecipitation, kinase assays, or phosphorylation site mapping are needed to clarify the precise biochemical relationship.

Mechanisms of CaMKIα-Mediated Regulation of the AMPK/SIRT3 Pathway in Inflammation Attenuation

Our findings indicate that CaMKIα knockdown restores p-AMPK and SIRT3 expression while suppressing pro-inflammatory mediators, including NF-κB, NLRP3, COX-2, and iNOS. Extensive evidence has demonstrated that AMPK activation protects against inflammatory lung injury by suppressing NF-κB signaling and NLRP3 inflammasome activity, enhancing autophagy, and limiting pro-inflammatory cytokine production, ultimately alleviating lung damage induced by LPS or sepsis [20–22]. SIRT3 has similarly been shown to confer anti-inflammatory protection in ALI and sepsis-associated lung injury, with its upregulation typically associated with inflammation suppression and initiation of repair responses [23,24]. Consistently, in our study, CaMKIα knockdown increased p-AMPK and SIRT3 levels, correlating with the observed anti-inflammatory phenotype. By relieving CaMKIα-mediated negative regulation, AMPK/SIRT3 signaling activity is restored, which inhibits NF-κB- and NLRP3-mediated inflammatory responses. Experiments using Compound C further confirmed the essential role of AMPK in mediating these protective effects [25,26].

Our findings expand current understanding of ALI pathology by identifying CaMKIα as an upstream modulator capable of the AMPK/SIRT3 axis, thereby linking calcium signaling to mitochondrial homeostasis and inflammatory control. This mechanistic connection has been insufficiently addressed in previous ALI research, which has primarily focused on downstream AMPK activation or SIRT3-mediated mitochondrial protection. Recent studies have emphasized the importance of upstream regulatory nodes that integrate metabolic stress and inflammatory signaling in lung injury, highlighting the relevance of our results in addressing this gap. By demonstrating that CaMKIα suppression alleviates inflammatory responses through AMPK/SIRT3-related pathways, our study provides both conceptual and mechanistic insights that may inform the development of targeted therapies for neonatal ALI.

Nevertheless, several limitations should be acknowledged. Compound C was selected because it is a widely used pharmacological AMPK inhibitor and has been validated in numerous ALI and inflammation-related studies to effectively suppress AMPK activation *in vitro* and *in vivo* [27,28]. However, it is not completely specific and may influence other kinases and metabolic pathways [29], which could contribute to off-target effects. Therefore, although our results strongly support a role for AMPK/SIRT3 activation in CaMKIα-mediated regulation of inflammatory responses, future studies employing more selective inhibitors or genetic approaches are required to confirm the pathway specificity. Additionally, our *in vitro* experiments were limited to alveolar type II epithelial L2 cells and did not account for the contributions of other key immune cell populations in ALI. Future studies could employ conditional CaMKIα and AMPK/SIRT3 knockout animal models and analyses across multiple time points and LPS doses to elucidate the dynamic regulation of this signaling network. Systematic investigations of cell type-specific effects, combined with transcriptomic and metabolomic analyses, would further clarify the downstream regulatory network of CaMKIα. From a translational perspective, small-molecule inhibitors

or gene-based strategies targeting CaMKIα may represent novel therapeutic approaches for ALI/ARDS. Combining these approaches with existing AMPK activators and SIRT3 agonists could further enhance their clinical potential.

Conclusion

In summary, our study demonstrates that CaMKIα contributes to inflammatory responses in acute lung injury by negatively regulating the AMPK/SIRT3 pathway. Knockdown of CaMKIα alleviates LPS-induced lung injury, reduces apoptosis, and suppresses pro-inflammatory cytokine production in neonatal rats and alveolar epithelial cells, largely through restoration of AMPK phosphorylation and SIRT3 expression. These findings reveal a novel upstream regulatory mechanism and suggest that targeting CaMKIα may represent a promising therapeutic strategy for ALI/ARDS.

Availability of Data and Materials

The analyzed data sets generated during the study are available from the corresponding author upon reasonable request.

Author Contributions

LNZ made substantial contributions to the conception and design of the study, acquisition, analysis, and interpretation of data, and drafted the original manuscript. BZ contributed substantially to data acquisition, investigation, data curation, and visualization, and participated in critical revision of the manuscript for important intellectual content. LZZ was responsible for validation, software implementation, and statistical analysis, and contributed to data interpretation and critical manuscript revision. PFZ contributed to the conception and design of the study, participated in data interpretation, supervised the project, and critically revised the manuscript for important intellectual content. All authors approved the final version to be published, and agreed to be accountable for all aspects of the work, ensuring that questions related to the accuracy or integrity of any part of the work are appropriately investigated and resolved.

Ethics Approval and Consent to Participate

All animal experiments were approved by the Experimental Animal Center of Wenzhou University (WZU-2024-296). All procedures were carried out in accordance with institutional ethical guidelines, with efforts made to minimize animal use and suffering.

Acknowledgment

The authors sincerely acknowledge Wenzhou University for providing the experimental facilities and for approving the animal experiments. Their support and cooperation were essential for the completion of this study.

Funding

This research was funded by the Science and Technology Program of Wenzhou (ID: Y20240156).

Conflict of Interest

The authors declare no conflict of interest.

References

[1] Kuldanek SA, Kelher M, Silliman CC. Risk factors, management and prevention of transfusion-related acute lung injury: a comprehensive update. Expert Review of Hematology. 2019; 12: 773–785. https://doi.org/10.1080/17474086.2019.1640599.

[2] Jia H, Sodhi CP, Yamaguchi Y, Lu P, Ladd MR, Werts A, *et al*. Toll Like Receptor 4 Mediated Lymphocyte Imbalance Induces Nec-Induced Lung Injury. Shock. 2019; 52: 215–223. https://doi.org/10.1097/SHK.0000000000001255.

[3] Yin TJ, Hu YS, Cheng S, Yong QJ. Dynamic changes of pulmonary arterial pressure in perinatal neonates with pulmonary and extrapulmonary acute lung injury/respiratory distress syndrome. Medicine. 2019; 98: e14830. https://doi.org/10.1097/MD.0000000000014830.

[4] Bellani G, Laffey JG, Pham T, Fan E, Brochard L, Esteban A, *et al*. Epidemiology, Patterns of Care, and Mortality for Patients With Acute Respiratory Distress Syndrome in Intensive Care Units in 50 Countries. JAMA. 2016; 315: 788–800. https://doi.org/10.1001/jama.2016.0291.

[5] Fan E, Brodie D, Slutsky AS. Acute Respiratory Distress Syndrome: Advances in Diagnosis and Treatment. JAMA. 2018; 319: 698–710. https://doi.org/10.1001/jama.2017.21907.

[6] Mokrá D. Acute lung injury - from pathophysiology to treatment. Physiological Research. 2020; 69: S353–S366. https://doi.org/10.33549/physiolres.934602.

[7] Zhao X, Zmijewski JW, Lorne E, Liu G, Park YJ, Tsuruta Y, *et al*. Activation of AMPK attenuates neutrophil proinflammatory activity and decreases the severity of acute lung injury. American Journal of Physiology. Lung Cellular and Molecular Physiology. 2008; 295: L497–L504. https://doi.org/10.1152/ajplung.90210.2008.

[8] Huang Q, Ren Y, Yuan P, Huang M, Liu G, Shi Y, *et al*. Targeting the AMPK/Nrf2 Pathway: A Novel Therapeutic Approach for Acute Lung Injury. Journal of Inflammation Research. 2024; 17: 4683–4700. https://doi.org/10.2147/JIR.S467882.

[9] Zhao W, Zhang L, Chen R, Lu H, Sui M, Zhu Y, *et al*. SIRT3 Protects Against Acute Kidney Injury via AMPK/mTOR-Regulated Autophagy. Frontiers in Physiology. 2018; 9: 1526. https://doi.org/10.3389/fphys.2018.01526.

[10] Chen J, Cai Y, Peng X, Xu Y, Chen L, Pan X, *et al*. Dexmedetomidine reduces acute lung injury caused by LPS through the SIRT3 signaling pathway *in vivo*. Frontiers in Pharmacology. 2025; 16: 1524219. https://doi.org/10.3389/fphar.2025.1524219.

[11] Guo L, Stripay JL, Zhang X, Collage RD, Hulver M, Carchman EH, *et al*. CaMKIα regulates AMP kinase-dependent, TORC-1-independent autophagy during lipopolysaccharide-induced

acute lung neutrophilic inflammation. Journal of Immunology. 2013; 190: 3620–3628. https://doi.org/10.4049/jimmunol.1102975.

[12] Wang K, Chen Y, Zhang P, Lin P, Xie N, Wu M. Protective Features of Autophagy in Pulmonary Infection and Inflammatory Diseases. Cells. 2019; 8: 123. https://doi.org/10.3390/cells8020123.

[13] Becker E, Jr, Husain M, Bone N, Smith S, Morris P, Zmijewski JW. AMPK activation improves recovery from pneumonia-induced lung injury via reduction of er-stress and apoptosis in alveolar epithelial cells. Respiratory Research. 2023; 24: 185. https://doi.org/10.1186/s12931-023-02483-6.

[14] Long ME, Mallampalli RK, Horowitz JC. Pathogenesis of pneumonia and acute lung injury. Clinical Science. 2022; 136: 747–769. https://doi.org/10.1042/CS20210879.

[15] Nguyen N, Xu S, Lam TYW, Liao W, Wong WSF, Ge R. ISM1 suppresses LPS-induced acute lung injury and post-injury lung fibrosis in mice. Molecular Medicine. 2022; 28: 72. https://doi.org/10.1186/s10020-022-00500-w.

[16] Xie R, Tan D, Liu B, Xiao G, Gong F, Zhang Q, *et al*. Acute respiratory distress syndrome (ARDS): from mechanistic insights to therapeutic strategies. MedComm. 2025; 6: e70074. https://doi.org/10.1002/mco2.70074.

[17] Bos LDJ, Ware LB. Acute respiratory distress syndrome: causes, pathophysiology, and phenotypes. Lancet. 2022; 400: 1145–1156. https://doi.org/10.1016/S0140-6736(22)01485-4.

[18] Huang Q, Le Y, Li S, Bian Y. Signaling pathways and potential therapeutic targets in acute respiratory distress syndrome (ARDS). Respiratory Research. 2024; 25: 30. https://doi.org/10.1186/s12931-024-02678-5.

[19] Sharp C, Millar AB, Medford ARL. Advances in understanding of the pathogenesis of acute respiratory distress syndrome. Respiration. 2015; 89: 420–434. https://doi.org/10.1159/000381102.

[20] Xu Y, Bai L, Yang X, Huang J, Wang J, Wu X, *et al*. Recent advances in anti-inflammation via AMPK activation. Heliyon. 2024; 10: e33670. https://doi.org/10.1016/j.heliyon.2024.e33670.

[21] Liu Y, Zhang Y, You G, Zheng D, He Z, Guo W, *et al*. Tangeretin attenuates acute lung injury in septic mice by inhibiting ROS-mediated NLRP3 inflammasome activation via regulating PLK1/AMPK/DRP1 signaling axis. Inflammation Research. 2024; 73: 47–63. https://doi.org/10.1007/s00011-023-01819-8.

[22] Li H, Nie Y, Hui H, Jiang X, Xie Y, Fu C. Activation of the AMPK/Nrf2 pathway ameliorates LPS-induced acute lung injury by inhibiting oxidative stress and reducing inflammation. Journal of Cardiothoracic Surgery. 2024; 19: 568. https://doi.org/10.1186/s13019-024-03020-2.

[23] Sun M, Li Y, Xu G, Zhu J, Lu R, An S, *et al*. Sirt3-Mediated Opa1 Deacetylation Protects Against Sepsis-Induced Acute Lung Injury by Inhibiting Alveolar Macrophage Pro-Inflammatory Polarization. Antioxidants & Redox Signaling. 2024; 41: 1014–1030. https://doi.org/10.1089/ars.2023.0322.

[24] Yan C, Lin X, Guan J, Ding W, Yue Z, Tang Z, *et al*. SIRT3 Deficiency Promotes Lung Endothelial Pyroptosis Through Impairing Mitophagy to Activate NLRP3 Inflammasome During Sepsis-Induced Acute Lung Injury. Molecular and Cellular Biology. 2025; 45: 1–16. https://doi.org/10.1080/10985549.2024.2426282.

[25] Jansen T, Kvandová M, Daiber A, Stamm P, Frenis K, Schulz E, *et al*. The AMP-Activated Protein Kinase Plays a Role in Antioxidant Defense and Regulation of Vascular Inflammation. Antioxidants. 2020; 9: 525. https://doi.org/10.3390/antiox9060525.

[26] Sun M, Wang F, Li H, Li M, Wang Y, Wang C, *et al*. Maresin-1 Attenuates Sepsis-Associated Acute Kidney Injury via Suppressing Inflammation, Endoplasmic Reticulum Stress and Pyroptosis by Activating the AMPK/SIRT3 Pathway. Journal of Inflammation Research. 2024; 17: 1349–1364. https://doi.org/10.2147/JIR.S442729.

[27] Li H, Zou Q, Wang X. Bisdemethoxycurcumin alleviates LPS-induced acute lung injury via activating AMPKα pathway. BMC Pharmacology & Toxicology. 2023; 24: 63. https://doi.org/10.1186/s40360-023-00698-3.

[28] Li W, Qiu X, Jiang H, Zhi Y, Fu J, Liu J. Ulinastatin inhibits the inflammation of LPS-induced acute lung injury in mice via regulation of AMPK/NF-κB pathway. International Immunopharmacology. 2015; 29: 560–567. https://doi.org/10.1016/j.intimp.2015.09.028.

[29] Park HY, Choi SH, Lee HS, Ko J, Yoon JS. Compound C exerts a therapeutic effect on Graves' orbitopathy via AMPK independent pathways. International Journal of Molecular Medicine. 2025; 55: 83. https://doi.org/10.3892/ijmm.2025.5524.